Subtropical Agriculture and Environments 72:29-36.2021

Identification of Flooding Risk Factors in Texas Citrus Production with UAV imagery: A Case Study

David A. Laughlin[1], Jorge Solorzano[2], Juan Enciso[2], and Veronica Ancona[1*]

[1]Texas A&M University Kingsville Citrus Center, 312 N. International Blvd, Weslaco, TX 78599, USA
[2]Texas A&M AgriLife Research, 2415 E. Business 83, Weslaco, TX 78596, USA

*Corresponding author email: veronica.ancona-contreras@tamuk.edu

ABSTRACT

In the fall of 2019, a panel of 6-year-old Rio Red grapefruit trees near Monte Alto, TX, began exhibiting wilting symptoms and tree decay. Interestingly, the surrounding Rio Red grapefruit panels of similar and different ages showed none of the symptoms observed in the affected panel. As the reason of tree decay was not apparent, this study aimed to investigate the underlying cause of orchard decline. Earlier in the summer, the area was affected by significant rain events that resulted in transient flooding of the affected and surrounding orchards, leading us to hypothesize that site conditions could be the culprit of tree decay. The affected panel (East) was compared to a healthy adjacent panel (West) to determine site characteristics that may have predisposed the East panel to collapse. We used an unmanned aerial vehicle (UAV) to monitor the decline in tree health measured as a reduction in triangular greenness index (TGI), and to evaluate topography differences between panels. Aerial images were captured six times in two different intervals from November 2019 and February 2020. Aerial images showed rapid tree decline in the affected East panel as measured in lower TGI values compared to the West panel($P<0.0001$). The elevation of the declined East panel averaged at 16.01 m above mean sea level (AMSL), and the healthy West panel was at 16.48 m AMSL. The depth of the phreatic water surface was 1.58 m below the soil level in the East panel and 2.83 m below the healthy West panel's soil level, a difference of 1.25 m. We also assessed *Phytophthora* spp. propagules, as this pathogen is associated with citrus root rot in the region. *Phytophthora* spp. propagule counts in both panels exceeded the 10 CFU/cm^3 treatment threshold for this pathogen. Lastly, historical rainfall records were analyzed and it was determined that the rain events preceding the orchard decline were abnormally high for the region. Therefore, we concluded that excessive rainfall in an area with lower elevation, poor drainage, and high phreatic water surface induced massive *Phytophthora* root rot, which led to a rapid tree decline and orchard collapse.

Additional index words: Flood irrigation; *Phytophthora*; soil-borne pathogens

---

Citrus is an important specialty crop in the United States with a total estimated value across varieties of US $ 3.35 billion during the 2018-19 season (USDA-NASS 2019). In Texas alone, the value of citrus produced ranged from $86.6 million in the 2016-17 season to $100.6 million in the 2017-18 season (USDA-NASS 2019). Out of the four U.S. citrus-producing states, Texas is the only state that has steadily increased its citrus acreage over the last few years (USDA-NASS 2019), and this trend is likely to continue.

Numerous biotic and abiotic factors limit citrus production throughout the world. Diseases such as *Phytophthora* foot rot (Chaudhary et al., 2020), *Fusarium* dry rot (Kunta et al., 2015), citrus Huanglongbing (da Graça et al., 2016), and citrus canker (Das, 2003) can limit production and reduce acreage. Abiotic factors such as soil salinity, drought, wind, sun damage, and flooding can impact both production and fruit quality (Adams et al., 2019; Freeman, 1976; Louzada et al., 2008). In particular, soil drainage is a problem for many citrus growers in the Rio Grande Valley (RGV) of South Texas (Maierhofer, 1947). Tools are required to aid growers in site selection for future orchards or adjusting management practices for current orchards.

The use of unmanned aerial vehicles (UAV) to detect crop stress and identify optimal field sites is a developing field in precision agriculture (Radoglou-Grammatikis et al., 2020). UAV imaging using red-green-blue (RGB) images versus costly thermal, infrared, or visible-near infrared cameras allows for a rapid and economically inexpensive evaluation method for potentially large land areas that can lead to swift and informed management decisions. Plant stress status can also be accurately measured using aerial RGB images by calculating the triangular greenness index (TGI), which is related to leaf chlorophyll content and

can be correlated to plant health (Garza et al., 2020). Topographical data can also be extracted from the same images and be used to take corrective action or as a survey tool during orchard planning and establishment.

In this communication, we report a case study in which, following a severe rain event in June of 2019, a panel of grapefruit trees in an orchard north of Monte Alto, Texas began to exhibit leaf curling and wilt symptoms during the fall of 2019. By January 2020, most of the trees had wilted and defoliated, and many had died, while the neighboring panels remained healthy. The primary objective of this study was to determine the cause of tree death and identify the factors that led to tree decline. We monitored tree decline over time using UAV imagery as compared to a neighboring healthy panel. UAV imagery, in-field measurements and analysis of historical rainfall patterns were used to identify site characteristics and significant rain events potentially responsible for orchard decline.

MATERIALS AND METHODS

Study Area. The study was conducted on a citrus orchard north of Monte Alto, Texas (26°23'5.63"N, -97°58'39.91"W, 16 m AMSL). The soil in this area is classified as a Willacy fine sandy loam characterized by a fine sandy loam in the top 35 cm and by a horizon of sandy clay loam from 35 to 180 cm, according to the USDA NRCS Soil Survey data. The 2.43 ha study site consisted of two adjacent panels planted with Rio Red grapefruit (*Citrus x paradisi* Macf.) grafted onto sour orange rootstock (*Citrus aurantium*). The west panel was planted in 2003, and the east panel was planted in 2013, both at a density of 359 trees/ha with a square layout with 3.6 m between trees and 7.6 m between rows.

Soil sampling, phreatic water surface determination, and historical precipitation data. Four different survey areas were selected to obtain soil samples and determine the phreatic water level. Site A was located in the northwest quadrant of a healthy panel, site B was located in the southeast quadrant of the same panel, site C was located in the northwest quadrant of the declining panel, and site D was located in the southeast quadrant of the declining panel (Figure 1). Soil samples were collected from each of the four different sites in the survey area at depths of 30, 60, 90, and 120 cm using a hand auger. Soil samples were analyzed for texture, pH, electroconductivity (EC), and nutrients (NO_3-N, K, Ca, Mg, S), and Na at the Texas A&M Soil, Water, and Forage Testing Laboratory, College Station, TX. The phreatic water surface was determined using a water level meter equipped with a Solinst 101 water level probe (Solinst Canada Ltd., Georgetown, ON, Canada), once in December of 2019 and again in June of 2020. Historical precipitation data was obtained from a local weather station monitored by Texas A&M AgriLife Research and Extension Center.

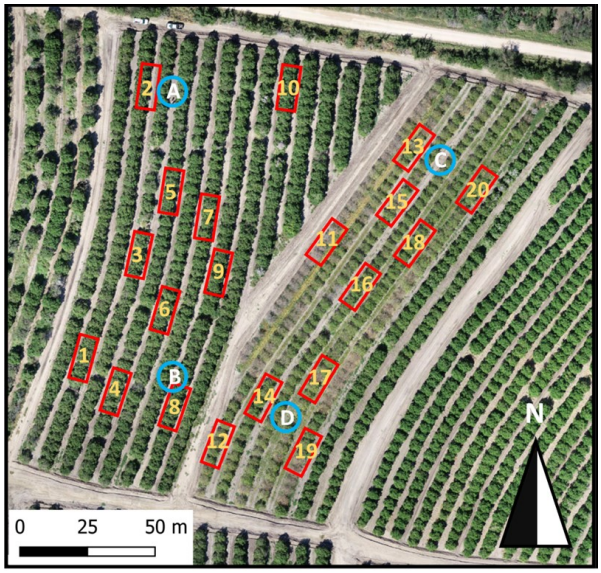

Fig. 1. Aerial view of the study area. Red boxes indicate area from where TGI and elevation data were extracted. Blue circles indicate sites (A-D) where the water table was determined, and where soil samples were taken for analysis.

Aerial Image Acquisition and Orthomosaic Generation. Images were acquired using a DJI Phantom 4 pro quadcopter (DJI, Shenzhen, China). The RGB sensor mounted on the Phantom 4 pro is equipped with a 20 Megapixels resolution and 1-inch CMOS (Complementary Metal Oxide Semiconductor) detector. Six flights were conducted to collect RGB images at 50 m altitude AGL with 75% frontal and side overlap to monitor tree decay for 3 months (November 1, November 18, December 4, and December 14 of 2019, January 17, and February 27 of 2020). Eight Ground Control Points (GCPs) were installed around the study area for precise geo-referencing and UAV data co-registration. The center coordinate of all GCP's was surveyed by using a Vmap Dual Frequency Post Processed Kinematic (PPK) GNSS Receiver (Micro Aerial Projects, Gainesville, FL). Raw images were processed using Agisoft Metashape Professional software (AgiSoft LLC, St. Petersburg, Russia) to generate orthomosaic images and digital elevation models. The coordinates of GCPs were input into the software for geo-referencing and co-registration of orthomosaics, achieving one cm level accuracy.

Image processing and analysis. Image analysis was performed using QGIS (Quantum Geographic Information System). Ten polygons encompassing five trees were generated for each panel to extract information from 50 trees per plot over time (Figure 1). The TGI index was generated for each polygon from the RGB orthomosaic. The TGI of each polygon was calculated using the raster calculator tool by applying the equation TGI = (RGREEN – (0.39 * RRED) – (0.61 * RBLUE))/(Normalized to the maximum value

of Red, Green and Blue bands (Hunt et al., 2011). The average TGI values within each polygon were extracted using the zonal statistics tool. The point sampling tool was applied to the digital elevation model to obtain the elevation from each polygon.

Pathogen enumeration. Sampling was performed to determine the presence of the two main soilborne pathogens that cause rapid citrus decline in Texas, *Phytophthora* spp. and *Fusarium* spp. Soil samples were collected from within the drip zone of five randomly selected trees in each of the two panels using a small handheld trowel. The soil samples were stored in plastic bags and processed within 24 hours. To enumerate propagules of *Fusarium* spp., 10g of each soil sample were suspended in 90 mL of ddH_2O and mixed well. One mL of the soil suspension was further diluted in 9 mL of ddH_2O and plated onto 10 plates of Fusarium selective medium II (FSMII) to calculate the number of propagules per g of soil (Dhingra and Sinclair, 1995). *Phytophthora* spp. propagules were enumerated as previously described (Timmer et al., 1988) and expressed as the number of propagules per cm^3 of soil. *Fusarium* spp. and *Phytophthora* spp. propagules were enumerated from the same soil samples. Two declined trees were uprooted with a backhoe, to assess root rot symptoms and samples of the roots were plated on FSMII and PARPH to determine if roots were colonized by *Fusarium* spp. or *Phytophthora* spp., respectively. The roots were also examined for signs of root damage by pests, such as root weevils, or other plant pathogens.

Statistical analysis. All analyses were executed using SAS statistical software (SAS version 9.4, SAS Inc., Cary, NC, USA). A T-test was performed to determine the difference in elevation, pathogen propagules, and soil texture between the east and west panels using the TTEST procedure. Pooled, Cochran, and Satterthwaite tests were calculated. The TGI for the two panels was analyzed as a general linear model (GLM) where the north sides and the south sides of the entire study were separated and analyzed as experimental blocks to account for block variation. Therefore, statistical analysis was performed as a multifactorial experiment, including block, location, and time as factors. The area under the curve (AUC) was obtained for each panel using the mean TGI over time. The AUC values were used as additional components for both the stepwise regressions and the correlation analysis. A stepwise regression analysis was performed to determine the most likely affected TGI AUC factors, TGI measured at the initial date, and TGI measured at the final date. The stepwise analysis was designed to accommodate the soil characteristics taken at four different depths. The soil composition variables included in the stepwise regression were pH, electroconductivity (EC), NO_3N, P, K, Ca, Mg, S, Na, % sand, % silt, % clay, water content (w/w), fall phreatic water level, summer phreatic water level, *Fusarium* spp. propagules/100 cm^3 soil, and *Phytophthora* spp. propagules/100 cm^3 soil. To compare against these variables, the lowest and the highest TGI values were eliminated from each panel. The analyses were performed using the REG procedure with the forward selection in the model statement to define the variables that most highly explain the effects on TGI. The correlation analysis was performed using the same data set using the CORR procedure. Historical rainfall data was analyzed using the Chi-square statistic feature of the FREQ procedure. The contribution of all dates analyzed were calculated using the CELLCHI2 option. The results were visualized using a correspondence analysis plot.

RESULTS

Site characteristics and pathogen enumeration. The soil type was classified as sandy clay loam, consistent with the NRCS Soil Survey data, which classified the soil as Willacy fine sandy loam. The only exception was the soil sample taken at site B at 30 cm depth, and two samples were taken at 30 and at 90 cm depths, all three of which were classified as a sandy loam (Supplemental Figure 1). There was no significant difference across sampling sites (P=.4385). There was no significant difference in the populations of *Fusarium* spp. (P=.6447) or *Phytophthora* spp. (P=.7497) between the two panels (Supplementary Table 1). The number of *Phytophthora* spp. propagules ranged from 0 to 72 propagules per cm^3 of soil, on average these populations fall above the treatment threshold of 10 propagules per cm^3 of soil (Graham and Menge, 1999). Root examination revealed symptoms consistent with the advanced stages of Phytophthora root rot, including destruction of the fibrous root system, sloughing off the cortex, and discoloration of the cambium (Timmer and Menge, 2001) (Figure 2).

Elevation and phreatic water surface differences. Elevations at sites A and B in the west panel were both 16.48 AMSL, while the elevations at sites C and D in the east panel were 15.93 and 16.09, respectively. Altitude differences between the two panels were sig-

Table 1. Stepwise regression comparing soil and site parameters against AUC for TGI.

Step	Variable	Variable #	Partial R-Square	Model R-Square	F Value	Pr > F
1	Elevation	1	0.5912	0.5912	20.25	0.0005
2	% Sand	2	0.1500	0.7412	7.54	0.0167
3	S	3	0.0457	0.7869	2.54	0.1347
4	Na	4	0.0183	0.8052	1.03	0.3316
5	N	5	0.0291	0.8343	1.76	0.2145

Fig. 2. Root rot symptoms sampled from declined (East) panel showing discoloration of the cambium (a) and complete degradation of the fibrous root system (b).

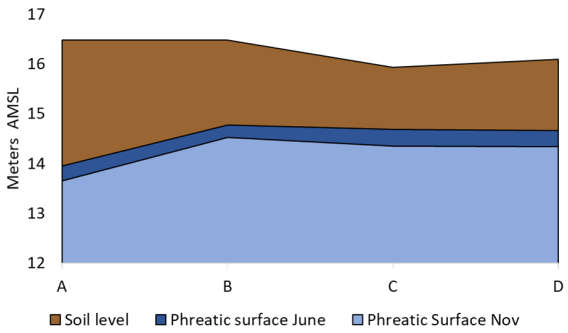

Fig. 3. Soil elevation and phreatic water surface in meters above the mean sea level (AMSL) of the four sampling sites in November 2019 and June 2020.

nificant (P≤.0001) for all three t-test methods used, pooled, Cochran, and Satterthwaite. The levels of the phreatic water surface between the west and east panel were more marked, with the phreatic water surface being measured at depths of 2.83 and 1.96 m at sites A and B, respectively, and 1.58 and 1.76 m at sites C and D, respectively, in November 2019 (Figure 3). Drainage problems are common in South Texas due to the shallow water tables and the proximity to the sea.

Although citrus tree roots grow in the first 45 cm of soil depth (Simpson et al., 2020), it is common for growers to install drain tile at a minimum soil depth of 2 m to drain excess water that accumulates just after irrigation or rainfall at shallower soil depths. The drain tiles discharge the water into an open ditch. This water is captured by larger collector drains which ultimately discharged the excess water into the Rio Grande River. Some citrus orchards, as was the case in both panels in the study area, do not have drain tiles, and this may be the reason for water depths of 1.58 and 1.76 m.

Monitoring tree decay with UAV imagery. TGI was used as a measure of tree decay. There was a significant difference in TGI over time (Figure 4; P<.0001) and between the west and east panels (P<.0001) as well as a significant interaction between time and location (P=.0168). Forward stepwise regression was performed against the calculated AUC for both panels to determine the parameters that had the greatest effect on TGI reduction. According to the analysis, five factors were identified that could potentially explain the decline observed. Elevation was the main factor contributing 59.12% at P=0.0005, followed by sand content of the soil (15.00%, P=0.016). Other factors were

Table 2. Correlation table showing the Pearson correlation coefficients between evaluated parameters and associated P values.

	AUC TGI	pH	NO3N	K	Ca	Mg	S	Na	Elevation	Phreatic Surface 1	Phreatic Surface 2
AUC TGI	1										
pH	-0.06083	1									
	0.8229										
NO3N	-0.20219	0.12014	1								
	0.4527	0.6576									
K	-0.29475	-0.16544	-0.18098	1							
	0.2678	0.5403	0.5024								
Ca	-0.19454	**0.68044**	0.12338	**-0.58662**	1						
	0.4703	**0.0037**	0.6489	**0.0169**							
Mg	0.02944	**-0.53225**	-0.31936	0.47928	-0.49353	1					
	0.9138	**0.0338**	0.2279	0.0603	0.052						
S	0.32514	**0.55706**	0.16478	0.1307	0.05131	0.06705	1				
	0.2191	**0.025**	0.542	0.6295	0.8503	0.8051					
Na	**0.50795**	0.48274	-0.32803	0.12031	0.05943	0.05555	**0.69012**	1			
	0.0446	0.0582	0.2148	0.6572	0.8269	0.8381	**0.0031**				
Elevation	**0.76891**	-0.0686	-0.34352	-0.15658	-0.13247	0.04331	0.14114	**0.62348**	1		
	0.0005	0.8007	0.1927	0.5625	0.6248	0.8735	0.6021	**0.0099**			
Phreatic Surface 1	**0.50083**	**-0.52897**	**-0.51455**	0.24348	-0.45787	**0.64938**	0.06576	0.33619	**0.60805**	1	
	0.0481	**0.0351**	**0.0414**	0.3635	0.0745	**0.0065**	0.8088	0.203	**0.0125**		
Phreatic Surface 2	**0.53603**	-0.50649	-0.53329	0.22696	-0.45583	**0.62767**	0.08052	0.37544	**0.64388**	**0.99796**	1
	0.0323	0.0453	0.0334	0.3979	0.076	**0.0092**	0.7669	0.1519	**0.0071**	**<.0001**	

Correlations with P≤0.05 are in bold.

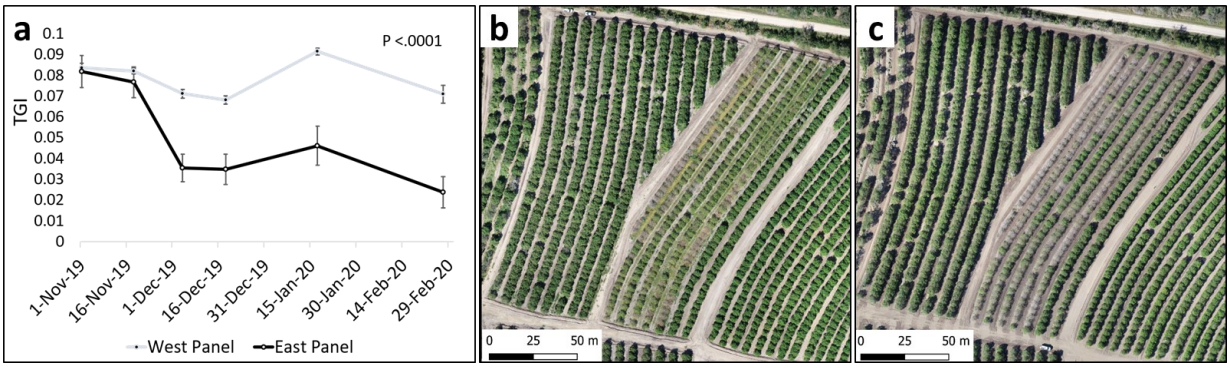

Fig. 4. Change in TGI from November 2019 to February 2020 between the west and east panels (a). Aerial images of the study area taken in November 2019 (b) and February 2020 (c) demonstrating the decline in the east panel overtime.

not statistically significant (Table 1). The TGI-AUC correlation analysis revealed four factors, elevation, both phreatic surface measurements, and Na were significantly correlated (P≤0.05, Table 2).

Analysis of historical rainfall data. Monthly rainfall was plotted from 2013 to 2019 to detect important rain events (Table 3). Chi-square analysis of rainfall data since 2013 broken down by month revealed significant (P≤.0001) Chi-square statistic, indicating that the rain events in October 2015 and June of 2018 and 2019 were significant. Contributions to the overall Chi-square statistic of 260.97 were 22.30 for October of 2015 and 48.35 and 12.88 for June of 2018 and 2019, respectively. June of 2018 contributed the highest percentages to the June column and the 2018 row Chi-square statistic by 41.09%, and 56.00%, respectively, while October of 2015 contributed the largest percentage to both the October column and the 2015 row, by 54.56% and 25.65%, respectively (Supplemental Table 2 and Supplemental Figure 2).

DISCUSSION

Many biotic and abiotic factors can affect plant health in the field. In many cases, these factors are not exclusive but rather interact in complex ways that impact the plant's overall health status. Poor drainage in citriculture systems can lead to loss of production, tree decline, and tree death. Factors that affect soil moisture and drainage include soil texture, irrigation management, cultural practices, water table depth, and site elevation. In this case study, we evaluated an orchard in the RGV of South Texas in which adjacent citrus panels displayed a dramatic difference in tree health. We utilized UAV imagery as a tool for tracking citrus

Table 3. Monthly rainfall records in cm near the study area showing precipitation patterns from 2013 to 2019.

Month/ Year	2013	2014	2015	2016	2017	2018	2019	Mean ± Std Error
January	3.51	2.11	5.64	3.28	0.97	1.14	2.08	2.67 ± 0.61
February	0.00	0.74	2.82	0.00	0.10	1.32	1.63	0.94 ± 0.40
March	0.00	3.71	9.40	6.32	4.55	0.20	7.19	4.48 ± 1.33
April	7.16	0.15	9.63	2.79	1.75	3.00	2.57	3.86 ± 1.25
May	2.92	8.53	10.31	6.17	7.42	2.01	3.28	5.81 ± 1.19
June	3.35	2.79	5.16	15.98	3.53	**38.66***	**24.61***	13.44 ± 5.23
July	1.83	1.85	2.69	0.00	1.52	0.25	0.30	1.21 ± 0.39
August	5.97	7.59	17.83	4.01	2.51	0.08	0.79	5.54 ± 2.29
September	19.30	25.27	17.63	5.66	17.30	13.87	10.62	15.66 ± 2.39
October	1.75	0.30	**29.31***	0.30	12.34	6.27	3.43	7.67 ± 3.95
November	9.30	9.75	3.02	4.75	2.39	1.30	4.70	5.03 ± 1.25
December	9.14	7.11	0.84	1.22	3.10	0.94	1.73	3.44 ± 1.26
Total (cm)	64.24	69.93	114.27	50.50	57.48	69.04	62.92	

* Significant contribution to Chi-square statistic

orchard decline and to identify topographical features that may predispose trees to flooding risk conditions. The rapid orchard decline observed was quantified by calculating the triangular greenness index (TGI) obtained by analyzing RGB aerial photographs, which has been previously shown to be a useful metric for the analysis of citrus tree health (Garza et al., 2020).

From the aerial images obtained, we were able to identify elevation differences between the two citrus panels. According to the analysis, soil elevation was the variable that contributed the most to the TGI AUC. However, following the correlation analysis, phreatic surface level, and elevation were significantly associated with TGI AUC. Interestingly, Na had a positive significant correlation with higher TGI AUC even though soil salinity levels were within acceptable ranges. In a previous study which examined the TGI spectral reflectance of citrus trees infected with HLB and Phytophthora foot rot, the authors discovered significant relationship between reduced TGI and increase levels of foliar Na compared to healthy trees (Garza et al., 2020). The authors proposed that perhaps uptake of Na was increased in diseased trees, which affected the TGI values, despite being under the toxicity threshold for Na. In the present study the foliar Na was not measured but the increased levels of soil Na in the healthy panel might lend support to the previous hypothesis that trees infected with *Phytophthora* spp. uptake more Na from the soil and thus result in lower Na in the soil. Further examination is warranted to study this potential relationship between Phytophthora infection and Na absorption.

Citrus trees in South Texas require roughly 100 cm of water annually, about half of which is provided by rainfall (Enciso et al., 2005). Farmers generally apply between 5 to 10 irrigations per year but the depth used per irrigation varies from farmer to farmer. However, most farmers apply between 10 to 20 cm per irrigation with the traditional flood irrigation method and they also apply at least one irrigation per month during the summer months. Farmers tend to overwater when water is abundant and cheap and water adequately during periods of drought when water restrictions are in place (Enciso et al. 2005; Nelson et al. 2011). In the study area, three irrigation events, greater than 6 cm each, were applied in June, July, and August, according to the farm manager responsible for study area. Because summer irrigation is a common practice and unlikely to be responsible for the orchard decline observed, we compared the rainfall patterns of 2018 and 2019 with those since 2013 to determine if there occurred rain events that were unusual for the region. Monthly rainfall data from 2013 to 2015 had higher total rainfall throughout the year but the distribution was more uniform, whereas in 2018 and 2019, much of the rain was concentrated in June and September. At the end of June in 2019 the RGV of South Texas experienced a rain event in which approximately 25 cm of precipitation led to flooding in most of the region. Thus, the study area received 35 to 45 cm of water within a period of a three weeks.

In citriculture, conducive conditions such as high soil moisture and high temperatures can lead to a sudden soilborne pathogen proliferation and outbreak of infection of susceptible host varieties (Timmer and Menge, 2001). *Fusarium spp.* and *Phytophthora spp*. cause dry root rot and root rot in citrus, respectively. Both pathogens have been reported in Texas citriculture (Kunta et al., 2015; Chaudhary el al., 2020) and depending on environmental factors, such as waterlogging, these pathogens can cause a rapid decline of citrus trees. The relationship between waterlogging and root rot induced by *Phytophthora* spp. has been studied in diverse perennial crop systems, including citrus. Several greenhouse studies have demonstrated that *Phytophthora cinnamomi* infection and waterlogging of avocado seedlings acted synergistically in plant death compared to either treatment independently (Ploetz and Schaffer, 1989; Reeksting et al., 2014). Similar greenhouse work have been performed in highbush blueberry (Silva et al., 1999), Fraser fir (Kenerley et al., 1984), and citrus (Chaudhary et al., 2016) that also demonstrate a positive correlation between *Phytophthora* infections and waterlogging. These Studies on perennial crops are typically limited to greenhouse experiments since in-field experiments are difficult to perform because they cannot control waterlogging, and in many cases the presence of *Phytophthora spp.* alone, without waterlogging, is usually not sufficient to cause significant disease.

The effect of waterlogging in combination with *Phytophthora spp.* is critical for the development of root rot and plant death. There are likely multiple interacting mechanisms that lead to the development of severe root rot including pathogen factors such as increased zoospore motility (Kenerley 1984) and host factors such as a reduction in stomatal conductance and subsequently reduced transpiration and assimilation of CO_2 (Ploetz and Schaffer, 1989; Rodríguez-Gamir et al., 2011). Tree age could also play a role in *Phytophthora* susceptibility under waterlogging conditions. Young growing trees that are developing their root system may succumb to waterlogging and disease, but once citrus trees reach maturity, the size and density of the root system is governed primarily by environmental conditions, rootstock variety, and agronomic management and not tree age (Morgan et al., 2007). In our study, although there were 10 years difference in tree age between the two panels, both were mature trees of productive age, therefore we believe that the reported observations are primarily the result of the discussed factors and not tree age.

Because waterlogging can lead to adverse effects on tree health and pathogen populations (*Fusarium* spp. and *Phytophthora* spp.) were high, we determined that the significant rainfall combined with excess irrigation triggered the rapid orchard decline observed in the east panel at the study area. The elevation and soil texture differences between the neighboring panels probably led to water accumulation in the lower (east)

panel resulting from water runoff, poor drainage, and high phreatic water surface, which are the ideal conditions for *Phytophthora* root rot infections to occur.

Although the relationship between *Phytophthora* root rot and high soil moisture is well studied in multiple systems, we believe that the current study provides field evidence that waterlogging can result from a combination of factors such as unusually high rainfall, application of unneeded irrigation and high phreatic water levels, which caused the collapse of a 6-year-old productive orchard by root rot. Moreover, this study also offers novel insight into the use of remote imagery for evaluating new planting sites and establishing potential risks related to waterlogging.

CONCLUSIONS

The results of this case study indicate that site characteristics related to topography and phreatic surface levels are correlated to the observed orchard decline. We also demonstrated that a significant rain event that occurred in July of 2019 that led to flood conditions, was likely to have triggered the decline of the grapefruit panel in the study area. Citrus growers could use UAV-based aerial surveys and RGB aerial imaging to identify flood-risk sections of otherwise healthy orchards to take corrective actions before tree decline occurs.

The use of imaging through UAV is rapidly becoming an indispensable tool in agriculture. Through UAV images, site characteristics can be determined that can help growers in site selection and site preparation. Field leveling is commonly used to direct the drainage of water, but implementation of raised beds in new orchards could help in reducing the risks associated with flooding and water logging (Simpson et al., 2020). Traditional agricultural systems would benefit from the use of modern technology such as UAV imaging and accurate soil moisture monitoring to transition into precision production systems and develop strategies to deal with unusual weather events and climate change (Sevier and Lee, 2004).

AUTHOR CONTRIBUTIONS

Project conceptualization and methodology, D.L., V.A., J.S., and J.E.; performed research and analyzed data, D.L. and J.S.; wrote the manuscript, D.L.; writing, reviewing, and editing the manuscript D.L., J.S., J.E., V.A. All authors have read and approve the final version of the manuscript.

ACKNOWLEDGMENTS

We want to thank Rio Farms Inc. and Matt Klosterman for facilitating this research. We also want to thank Ayrton Laredo for assisting in field data collection. This project was supported with funds from the Texas Citrus Producers Board to VA, the Ag Water Conservation grant from the Texas Water Development Board, the USDA-NIFA, grant number 554772, and the Hatch project "Development of Engineering Tools for Soil and Water Conservation," accession number 1016863.

LITERATURE CITED

Adams, S. N., Ac-Pangan, W. O., and Rossi, L. 2019. Effects of soil salinity on citrus rootstock 'US-942'' physiology and anatomy. HortScience. 54:787–792.

Chaudhary, S., Kusakabe, A., Melgar, J.C., 2016. Phytophthora infection in flooded citrus trees reduces root hydraulic conductance more than under non-flooded condition. Sci. Hortic. 202, 107–110.

Chaudhary, S., Laughlin, D. A., Setamou, M., da Graça, J. V, Kunta, M., Alabi, O. J., et al. 2020. Incidence, severity, and characterization of Phytophthora foot rot of citrus in Texas and implications for disease management. Plant Dis. 104:2455–2461.

da Graça, J. V., Douhan, G. W., Halbert, S. E., Keremane, M. L., Lee, R. F., Vidalakis, G., et al. 2016. Huanglongbing: An overview of a complex pathosystem ravaging the world's citrus. J. Integr. Plant Biol. 58:373–387.

Das, A. K. 2003. Citrus canker - a review. J. Appl. Hortic. 05:52–60.

Dhingra, O. D., Sinclair, J. B. 1995. *Basic Plant Pathology Methods*, 2nd ed.; CRC Lewis Publishers

Dlamini, S. N., Beloconi, A., Mabaso, S., Vounatsou, P., Impouma, B., and Fall, I. S. 2019. Review of remotely sensed data products for disease mapping and epidemiology. Remote Sens. Appl. Soc. Environ. 14:108–118.

Enciso, J., Sauls, J., Wiedenfeld, B., and Nelson, S. 2005. Irrigation of Citrus in Texas - A Review. Subtrop. Plant Sci. 57:16–22.

Freeman, B. 1976. Artificial windbreaks and the reduction of windscar of Citrus. Proc. Fla. State Hort. Soc. 89:52–54.

Garza, B. N., Ancona, V., Enciso, J., Perotto-Baldivieso, H. L., Kunta, M., and Simpson, C. 2020. Quantifying citrus tree health using true color UAV images. Remote Sens. 12:1–13.

Graham, J. H., Menge, J. A., 1999. Root Diseases, in: Timmer, L.W., Duncan, L.W. (Eds.), *Citrus Health Management.* St. Paul, MN. APS Press, pp.126-135.

Hunt, E. R.; Daughtry, C. S. T.; Eitel, J. U. H.; Long, D. S. 2011. Remote Sensing Leaf Chlorophyll Content Using a Visible Band Index. Agron. J. 103 (4): 1090—1099.

Kenerley, C.M., Papke, K., Bruck, R.I., 1984. Effect of Flooding on Development of Phytophthora Root Rot in Fraser Fir Seedlings. Phytopathology 74, 401–404.

Kunta, M., Salas, B., Gonzales, M., da Graca, J. V., 2015. First report on citrus dry rot in sour orange rootstock in Texas. J. Citrus Pathol. 4:98–104.

Louzada, E. S., Del Rio, H. S., Sétamou, M., Watson, J. W., Swietlik, D. M., 2008. Evaluation of citrus rootstocks for the high pH, calcareous soils of South Texas. Euphytica. 164:13–18.

Maierhofer, C. R., 1947. Drainage problems in the Rio Grande Valley. J. Rio Gd. Hortic. Soc. 2:22–29.

Morgan, K.T., Obreza, T.A., Scholberg, J.M.S., 2007. Orange tree fibrous root length distribution in space and time. J. Am. Soc. Hortic. Sci. 132, 262–269.

Nelson, S. D., Young, M., Enciso, J. M., Klose, S. L., Setamou, M., 2011. Impact of irrigation method on water saving and 'Rio Red' grapefruit packout in South Texas. Subtrop. Plant Sci. 63:14-22.

Ploetz, R.C., Schaffer, B., 1989. Effects of flooding and Phytophthora root rot on net gas exchange and growth of avocado. Phytopathology, 79, 204–208.

Radoglou-Grammatikis, P., Sarigiannidis, P., Lagkas, T., Moscholios, I., 2020. A compilation of UAV applications for precision agriculture. Comput. Networks. 172:107148

Reeksting, B.J., Taylor, N.J., Berg, N. Van Den, 2014. Flooding and *Phytophthora cinnamomi* : effects on photosynthesis and chlorophyll fluorescence in shoots of non-grafted *Persea americana* (Mill.) rootstocks differing in tolerance to Phytophthora root rot. South African J. Bot. 95, 40–53.

Rodríguez-Gamir, J., Ancillo, G., González-mas, M.C., Primo-Millo, E., Iglesias, D.J., Forner-Giner, M.A., 2011. Root signalling and modulation of stomatal closure in flooded citrus seedlings. Plant Physiol. Biochem. 49, 636–645.

Sevier, B., & Lee, W. 2004. Precision Agriculture in Citrus: A Probit Model Analysis for Technology Adoption. ASAE Paper No. 041092. St. Joseph, Mich.: ASAE.

Silva, A. De, Patterson, K., Rothrock, C., Mcnew, R., 1999. Phytophthora Root Rot of Blueberry Increases with Frequency of Flooding. HortScience 34, 693–695.

Simpson, C. R., Gonzales III, J., Enciso, J., Nelson, S. D., Sétamou, M., 2020. Root distribution and seasonal fluctuations under different grove floor management systems in citrus. Sci. Hortic. 272 (1): 109364.

Timmer, L. W., Menge, J. A., 2001. Diseases caused by *Phytophthora*, in : Timmer, L.W., Garnsey, S. M., Graham, J. H. (Eds.), *Compendium of Citrus Diseases.* St. Paul, MN. APS Press, pp. 12–15.

Timmer, L. W., Sandler, H. A., Graham, J. H., and Zitko, S. E. 1988. Sampling citrus orchards in Florida to estimate populations of *Phytophthora parasitica*. Phytopathology 78:940-94.

USDA-NASS. 2019. Citrus Fruits 2019. Summary. USDA, National Agricultural Statistics Service. Available online at https://www.nass.usda.gov/Publications/Todays_Reports/reports/cfrt0818.pdf

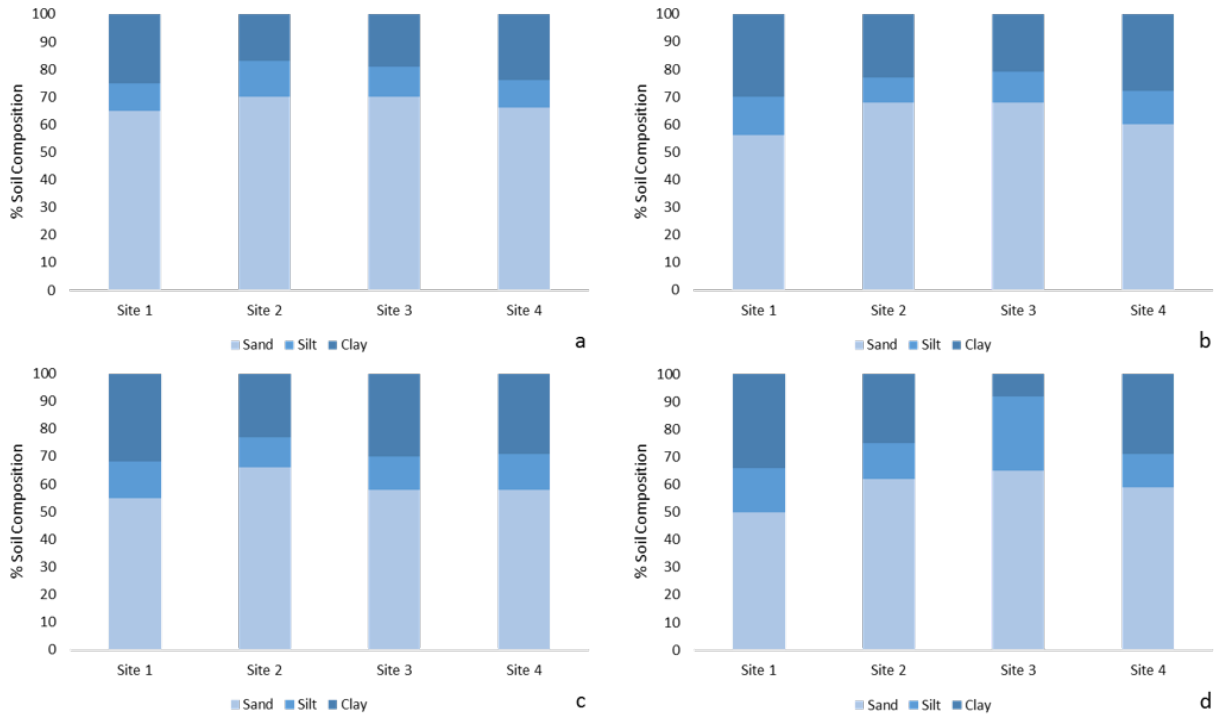

Supplementary Figure S1. Soil texture analysis at different soil depths. (a) 30 cm, (b) 60 cm, (c) 90 cm, and (d) 120 cm soil depths.

Supplementary Table 1. Soil propagule quantification in the study area.

Block	Row	Tree	*Fusarium* propagules/ 100cm³ soil	*Phytophthora* propagules/ 100cm³ soil
West	9	8	405	0
West	5	25	316	23
West	2	5	95	0
West	6	10	252	19
West	3	7	279	6
East	6	12	256	0
East	4	27	150	0
East	3	7	327	0
East	2	10	180	1
East	7	5	289	72

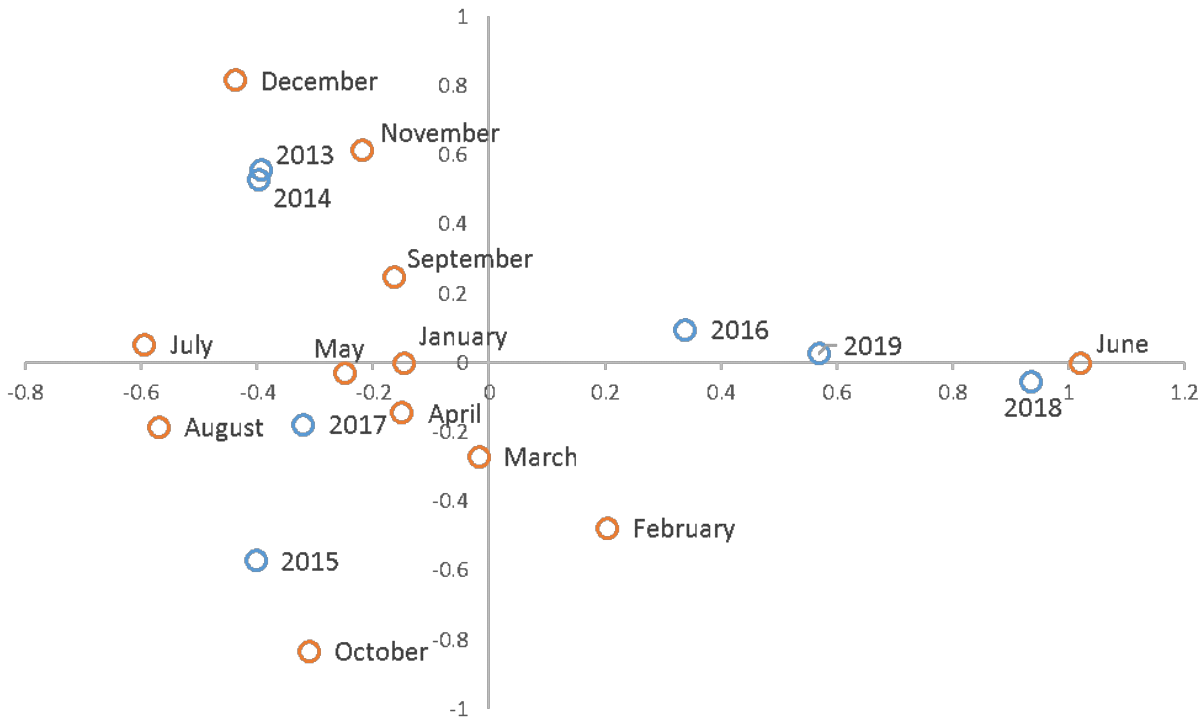

Supplementary Figure S2. Correspondence analysis demonstrating the nonindependence of rainfall in June 2018 and 2019 based on the significant Chi-square statistic.

Supplementary Table 2. Chi-square statistic from rainfall records in cm near the study area showing precipitation patterns from 2013 to 2019.

		April	August	December	February	January	July	June	March	May	November	October	September	Total
2013	**Frequency**	7.16	5.97	9.14	0.00	3.51	1.83	3.35	0.00	2.92	9.30	1.75	19.30	64.24
	Cell Chi-Square	3.65	0.15	11.28	0.87	0.44	0.46	6.58	4.13	1.10	4.70	4.00	1.65	
	Row %	11.15	9.29	14.23	0.00	5.46	2.85	5.22	0.00	4.55	14.47	2.73	30.05	
	Column %	26.48	15.39	37.97	0.00	18.72	21.62	3.56	0.00	7.19	26.41	3.26	17.60	
2014	**Frequency**	0.15	7.59	7.11	0.74	2.11	1.85	2.79	3.71	8.53	9.75	0.30	25.27	69.93
	Cell Chi-Square	3.57	0.75	3.89	0.05	0.12	0.34	8.46	0.14	1.27	4.41	7.09	5.84	
	Row %	0.22	10.86	10.17	1.05	3.01	2.65	4.00	5.30	12.20	13.95	0.44	36.14	
	Column %	0.56	19.58	29.54	11.15	11.26	21.92	2.97	11.82	21.00	27.71	0.57	23.05	
2015	**Frequency**	9.63	17.83	0.84	2.82	5.64	2.69	5.16	9.40	10.31	3.02	29.31	17.63	114.28
	Cell Chi-Square	1.72	8.45	4.08	1.05	0.36	0.26	12.91	0.58	0.07	3.30	22.30	2.51	
	Row %	8.42	15.60	0.73	2.47	4.93	2.36	4.51	8.22	9.02	2.65	25.65	15.43	
	Column %	35.59	45.97	3.48	42.69	30.12	31.83	5.48	29.96	25.38	8.59	54.56	16.08	
2016	**Frequency**	2.79	4.01	1.22	0.00	3.28	0.00	15.98	6.32	6.17	4.75	0.30	5.66	50.50
	Cell Chi-Square	0.00	0.00	0.65	0.68	0.93	0.87	4.01	2.93	0.92	0.34	4.96	2.84	
	Row %	5.53	7.95	2.41	0.00	6.49	0.00	31.64	12.53	12.22	9.41	0.60	11.22	
	Column %	10.33	10.35	5.06	0.00	17.50	0.00	16.98	20.16	15.19	13.49	0.57	5.17	
2017	**Frequency**	1.75	2.51	3.10	0.10	0.97	1.52	3.53	4.55	7.42	2.39	12.34	17.30	57.48
	Cell Chi-Square	0.64	0.92	0.02	0.59	0.70	0.28	5.14	0.20	1.45	0.74	5.73	1.49	
	Row %	3.05	4.37	5.39	0.18	1.68	2.65	6.14	7.91	12.90	4.15	21.48	30.09	
	Column %	6.48	6.48	12.87	1.54	5.16	18.02	3.75	14.49	18.25	6.78	22.98	15.77	
2018	**Frequency**	3.00	0.08	0.94	1.32	1.14	0.25	38.66	0.20	2.01	1.30	6.27	13.87	69.04
	Cell Chi-Square	0.18	5.33	1.78	0.16	0.85	0.74	48.35	4.04	2.43	2.72	0.23	0.17	
	Row %	4.34	0.11	1.36	1.91	1.66	0.37	56.00	0.29	2.91	1.88	9.09	20.09	
	Column %	11.08	0.20	3.90	20.00	6.11	3.00	41.09	0.65	4.94	3.68	11.68	12.65	
2019	**Frequency**	2.57	0.79	1.73	1.63	2.08	0.30	24.61	7.19	3.28	4.70	3.43	10.62	62.92
	Cell Chi-Square	0.24	3.55	0.61	0.71	0.04	0.57	12.88	2.45	0.73	0.01	1.76	0.87	
	Row %	4.08	1.25	2.75	2.58	3.31	0.48	39.12	11.43	5.21	7.47	5.45	16.88	
	Column %	9.48	2.03	7.17	24.62	11.13	3.60	26.16	22.91	8.06	13.35	6.38	9.68	
Total		27.05	38.79	24.08	6.60	18.72	8.46	94.08	31.37	40.64	35.20	53.72	109.65	488.37